Activation of SF1 Neurons in the Ventromedial Hypothalamus by DREADD Technology Increases Insulin Sensitivity in Peripheral Tissues

Eulalia A. Coutinho,[1,2] Shiki Okamoto,[1,2] Ayako Wendy Ishikawa,[2,3] Shigefumi Yokota,[1] Nobuhiro Wada,[4,5] Takahiro Hirabayashi,[4] Kumiko Saito,[1] Tatsuya Sato,[1] Kazuyo Takagi,[1,6] Chen-Chi Wang,[2,7] Kenta Kobayashi,[2,8] Yoshihiro Ogawa,[9,10,11] Seiji Shioda,[4] Yumiko Yoshimura,[2,3] and Yasuhiko Minokoshi[1,2]

Diabetes 2017;66:2372–2386 | https://doi.org/10.2337/db16-1344

The ventromedial hypothalamus (VMH) regulates glucose and energy metabolism in mammals. Optogenetic stimulation of VMH neurons that express steroidogenic factor 1 (SF1) induces hyperglycemia. However, leptin acting via the VMH stimulates whole-body glucose utilization and insulin sensitivity in some peripheral tissues, and this effect of leptin appears to be mediated by SF1 neurons. We examined the effects of activation of SF1 neurons with DREADD (designer receptors exclusively activated by designer drugs) technology. Activation of SF1 neurons by an intraperitoneal injection of clozapine-*N*-oxide (CNO), a specific hM3Dq ligand, reduced food intake and increased energy expenditure in mice expressing hM3Dq in SF1 neurons. It also increased whole-body glucose utilization and glucose uptake in red-type skeletal muscle, heart, and interscapular brown adipose tissue, as well as glucose production and glycogen phosphorylase *a* activity in the liver, thereby maintaining blood glucose levels. During hyperinsulinemic-euglycemic clamp, such activation of SF1 neurons increased insulin-induced glucose uptake in the same peripheral tissues and tended to enhance insulin-induced suppression of glucose production by suppressing gluconeogenic gene expression and glycogen phosphorylase *a* activity in the liver. DREADD technology is thus an important tool for studies of the role of the brain in the regulation of insulin sensitivity in peripheral tissues.

The ventromedial hypothalamus (VMH) plays a key role in the control of energy homeostasis (1) and glucose metabolism (2,3). Electrical stimulation of the VMH was thus found many years ago to increase glucose production by the liver (4). Expression of steroidogenic factor 1 (SF1), also known as adrenal 4 binding protein (AD4BP), defines a specific subset of VMH neurons (5–7). Genetic disruption of glutamate release from SF1 neurons in mice attenuated recovery from insulin-induced hypoglycemia, suggesting that glutamatergic SF1 neurons are responsible for the ability of the VMH to increase the blood glucose concentration (8). Electromagnetic manipulation also showed that activation of the transient receptor potential vanilloid 1 (TRPV1) ion channel in glucokinase (GK)-expressing neurons of the VMH elicited

[1]Division of Endocrinology and Metabolism, Department of Homeostatic Regulation, National Institute for Physiological Science, National Institutes of Natural Sciences, Okazaki, Aichi, Japan
[2]Department of Physiological Science, School of Life Sciences, SOKENDAI (The Graduate University for Advanced Studies), Hayama, Kanagawa, Japan
[3]Division of Visual Information Processing, Department of Fundamental Neuroscience, National Institute for Physiological Sciences, National Institutes of Natural Sciences, Okazaki, Aichi, Japan
[4]Global Research Center for Innovative Life Science, Hoshi University School of Pharmacy and Pharmaceutical Sciences, Tokyo, Japan
[5]Department of Diabetes and Metabolic Diseases, Graduate School of Medicine, The University of Tokyo, Tokyo, Japan
[6]Department of Human Life Science, Nagoya University of Economics, Inuyama, Aichi, Japan
[7]Center for Experimental Animals, National Institutes of Natural Sciences, Okazaki, Aichi, Japan
[8]Section of Viral Vector Development, Center for Genetic Analysis of Behavior, National Institute for Physiological Sciences, National Institutes of Natural Sciences, Okazaki, Aichi, Japan
[9]Department of Molecular Endocrinology and Metabolism, Graduate School of Medical and Dental Sciences, Tokyo Medical and Dental University, Tokyo, Japan
[10]Department of Medicine and Bioregulatory Science, Graduate School of Medical Sciences, Kyushu University, Fukuoka, Japan
[11]Japan Agency for Medical Research and Development, CREST (AMED-CREST), Tokyo, Japan

Corresponding author: Yasuhiko Minokoshi, minokosh@nips.ac.jp.

Received 2 November 2016 and accepted 8 June 2017.

This article contains Supplementary Data online at http://diabetes.diabetesjournals.org/lookup/suppl/doi:10.2337/db16-1344/-/DC1.

a hyperglycemic response (9), whereas optogenetic stimulation of SF1 neurons via channelrhodopsin 2 (ChR2) induced hyperglycemia and enhanced the counterregulatory response to glucopenia (10).

In contrast to such elicitation of a hyperglycemic response, the VMH has been found to increase glucose utilization and insulin sensitivity in some peripheral tissues. Electrical stimulation of the VMH increases glucose utilization in interscapular brown adipose tissue (BAT), heart, and skeletal muscle, but not in white adipose tissue (WAT), and induces hepatic glucose production (11). Leptin, which increases the activity of a subset of SF1 neurons in the VMH (12–14), also promotes both glucose uptake in peripheral tissues, including red-type skeletal muscle, and endogenous glucose production and thereby maintains blood glucose levels (15–17). Under hyperinsulinemic-euglycemic clamp conditions, leptin acting via the VMH enhanced both insulin-induced glucose utilization in some peripheral tissues, including red-type skeletal muscle, and suppression of hepatic glucose production (17). The VMH contains a heterogeneous population of neurons. A subset of VMH neurons expresses the long form of the leptin receptor (18), and most of these neurons also express SF1 (12,19). Whereas SF1 neurons in the VMH are required for maintenance of normal glucose and energy metabolism (20–22) and mediate the anorexic and metabolic effects of leptin (12,19,23,24), specific activation of leptin receptor–expressing neurons in the VMH by optogenetic stimulation of ChR2 did not induce hyperglycemia (10).

DREADD (designer receptors exclusively activated by designer drugs) technology allows spatial and temporal control of the activity of specific neurons. The hM3Dq designer receptor activates signaling by the G protein Gq, and its expression and activation in SF1 neurons of the VMH may therefore have effects on glucose and energy metabolism distinct from those of optogenetic stimulation via ChR2 (25). In the current study, we activated SF1 neurons in the VMH of mice via hM3Dq. Such activation increased whole-body glucose utilization, glucose uptake in some peripheral tissues—including red-type skeletal muscle, heart, and BAT—as well as endogenous glucose production and glycogen phosphorylase *a* activity in the liver, thereby maintaining blood glucose levels. During a hyperinsulinemic-euglycemic clamp, activation of SF1 neurons by hM3Dq increased insulin-induced glucose uptake in the same peripheral tissues and tended to enhance insulin-induced suppression of endogenous glucose production. In addition, activation of SF1 neurons by DREADD technology suppressed food intake and increased energy expenditure.

RESEARCH DESIGN AND METHODS

Animals

SF1-Cre recombinase (SF1-Cre) transgenic mice (Stock Tg [Nr5a1-cre] 7Lowl/J) were obtained from The Jackson Laboratory (Bar Harbor, ME) (12). Heterozygous transgenic mice were crossed with FVB/N Jcl mice (Clea, Tokyo, Japan), and the genotype of the resulting offspring was determined by PCR analysis (see Supplementary Table 1 for primer sequences). Mice were housed individually in plastic cages at 24° ± 2°C with lights on from 0600 to 1800 h and were given free access to laboratory chow (CE-2 diet, Clea) and water. All experiments were performed at the same room temperature and under the same light-dark cycle. Only male SF1-Cre or wild-type (WT) mice (12–16 weeks of age) were used in the current study. All animal experiments were performed in accordance with institutional guidelines for the care and handling of experimental animals and were approved by the National Institutes of Natural Sciences Institutional Animal Care and Use Committee (Okazaki, Japan).

Surgical Procedures

Stainless steel cannulas were implanted bilaterally into the VMH of WT or SF1-Cre mice at 12–14 weeks of age, as described previously (17). The stereotaxic coordinates for the position of the VMH (anterior to posterior position, 1.32 mm caudal to the bregma; height, 5.72 mm below the surface of the skull; lateral, 0.3 mm lateral to the bregma on each side) were obtained from the Mouse Brain Atlas (26). For measurement of 2-deoxyglucose (2DG) uptake and hyperinsulinemic-euglycemic clamp analysis, self-made polyethylene-silicone catheters were surgically implanted into the right jugular vein and carotid artery 3 days before experiments (17).

Preparation and Injection of an Adeno-Associated Virus Vector and Administration of Clozapine-*N*-Oxide

Two weeks after cannula implantation, 500 nL (1.9×10^{10} copies $\cdot$ μL^{-1}) of an adeno-associated virus (AAV, serotype 2) encoding AAV-hSyn-DIO-hM3Dq-mCherry-WPRE (AAV-hM3Dq) (25,27) were injected into each side of the VMH of SF1-Cre mice at a rate of 50 nL/min with the use of a pump (to yield SF1-Cre:AAV-hM3Dq mice). The DREADD plasmid is based on the FLEx (FLip-Excision) Switch system, which relies on two pairs of heterotypic, anti-parallel loxP-type recombination sites to achieve Cre-mediated transgene inversion and expression of an hM3Dq-mCherry fusion protein under the control of the mouse synapsin 1 gene promoter. It was obtained from B. L. Roth (25,27) and was expanded and packaged with the use of an AAV helper-free packaging system (Cell Biolabs, San Diego, CA). Mice were used for experiments 2 weeks after infection. With the exception of hyperinsulinemic-euglycemic clamp experiments, clozapine-*N*-oxide (CNO; 3 mg $\cdot$ kg^{-1}) (Enzo Life Sciences, Farmingdale, NY) was injected intraperitoneally into SF1-Cre:AAV-hM3Dq mice to activate the DREADD receptor hM3Dq, with PBS (saline) being injected into the same mice on a different day as a control. Half of the mice were injected first with saline and others with CNO, with there being no difference in the effects of CNO between mice injected first with CNO or with saline. For hyperinsulinemic-euglycemic clamp analysis, CNO (3 mg $\cdot$ kg^{-1}) or saline was injected into SF1-Cre:AAV-hM3Dq mice through a jugular vein catheter. Preliminary experiments showed that injection of a low

dose (0.3 mg · kg^{-1}) of CNO had no effect on food intake or whole-body glucose metabolism in SF1-Cre:AAV-hM3Dq mice (data not shown). Furthermore, the effects of bilateral injection of CNO (30 μmol/L; 1.5 pmol in 50 nL physiological saline) into the VMH on food intake and in an insulin tolerance test (ITT) were similar to those of an intraperitoneal injection. We therefore adopted intraperitoneal or intravenous injection of CNO (3 mg · kg^{-1}). To examine whether hM3Dq is expressed in SF1 neurons in a Cre recombinase-dependent manner, we also injected AAV-hM3Dq into the VMH of WT mice (WT:AAV-hM3Dq mice).

Immunofluorescent Analysis of hM3Dq-mCherry and cfos Expression

To validate the activation of SF1 neurons by hM3Dq in vivo, AAV-hM3Dq was unilaterally infected into the VMH of SF1-Cre mice. The contralateral side of the VMH was used as a control in the same mice. Mice were injected intraperitoneally with CNO 2 weeks after the infection, and 60 min later, mice were anesthetized with ketamine and xylazine and perfused transcardially with 4% paraformaldehyde in 0.1 mol/L phosphate buffer. Brain tissue was removed, fixed again, and embedded in optimal cutting temperature compound (Sakura Finetechnical, Tokyo, Japan). Serial cryosections (7 μm thick) were exposed to 10% normal horse serum (Santa Cruz Biotechnology, Dallas , TX) for 1 h at room temperature, and incubated first overnight at 4°C with rabbit polyclonal antibodies for cfos (1:200 dilution; Santa Cruz Biotechnology) and then for 90 min at room temperature with Alexa 488–labeled donkey antibodies for rabbit immunoglobulin G (1:400; Life Technologies). To validate endogenous fluorescence of mCherry in SF1-Cre:AAV-hM3Dq and WT:AAV-hM3Dq mice, those mice were also deeply anesthetized and perfused transcardially with 4% paraformaldehyde in 0.1 mol/L phosphate buffer. Fluorescence of mCherry and Alexa 488 was detected by a fluorescence microscope (AX-70; Olympus, Tokyo, Japan).

Basal Blood Glucose Concentration and Intraperitoneal Glucose Tolerance Test and ITT Analyses

To examine the effect of activation of SF1 neurons in the VMH on basal blood glucose levels, we deprived SF1-Cre:AAV-hM3Dq mice of food for 3 h and then injected them intraperitoneally with saline or CNO at time t = 0. Blood was collected from the tail vein at the indicated times for measurement of blood glucose concentration with the use of a OneTouch Ultra glucometer (LifeScan Japan, Johnson & Johnson, Tokyo, Japan). For the glucose tolerance test (GTT), SF1-Cre:AAV-hM3Dq mice were deprived of food overnight for 16 h and then injected intraperitoneally first with saline or CNO at t = −180 min and then with glucose (2 g · kg^{-1}) at t = 0. Blood glucose and plasma insulin concentrations were measured with the use of a OneTouch Ultra glucometer and an insulin ELISA kit (Shibayagi, Gunma, Japan). For the ITT, SF1-Cre:AAV-hM3Dq mice were deprived of food immediately before intraperitoneal injection with saline or CNO at t = −180 min. They were injected intraperitoneally with insulin (1 unit · kg^{-1}) (Sigma-Aldrich Japan, Tokyo, Japan) at t = 0, and the blood glucose concentration was measured at the indicated times.

Hyperinsulinemic-Euglycemic Clamp and 2DG Uptake

A hyperinsulinemic-euglycemic clamp was imposed, and 2DG uptake was measured in conscious and free-moving mice as previously described (17). Jugular vein and carotid artery catheters were connected to an infusion pump and a saline-filled syringe, respectively, at 4 h before the start of the experiment, after which time only water was available. CNO (3 mg · kg^{-1}) or saline was injected through the jugular vein catheter at t = −180 min in SF1-Cre:AAV-hM3Dq mice. A priming dose (5 μCi) of [3-^{3}H]glucose (American Radiolabeled Chemicals, St. Louis, MO) was also administered via the jugular vein catheter at t = −120 min and was followed by infusion of the tracer at a rate of 0.05 μCi · min^{-1} until the end of the experiment. Beginning at t = 0, corresponding to the steady-state condition, bovine insulin (Sigma-Aldrich Japan) was infused continuously (bolus of 16 mU · kg^{-1}, followed by a rate of 2.5 mU · kg^{-1} · min^{-1}) through the jugular vein catheter. Blood was collected from the carotid artery catheter, and blood glucose was monitored with the use of a OneTouch Ultra glucometer. Glucose (30%, wt/vol) was infused at a variable rate via the jugular vein catheter to maintain the blood glucose concentration at 100 mg · dL^{-1}. Withdrawn erythrocytes were suspended in sterile 0.9% saline and returned to each animal.

For assessment of 2DG uptake during the basal period, mice were infused with 2-[^{14}C]DG (5 μCi) (American Radiolabeled Chemicals) through the jugular vein catheter at t = −45 min. At t = −180, −45, −40, −30, −20, −10, and 0 min, arterial blood samples (50 μL) were collected for assessment of blood glucose R_a and R_d, which reflect endogenous glucose production and whole-body glucose utilization, respectively, as well as of 2DG uptake. For measurement of 2DG uptake during the clamp period, another group of mice was infused with 2-[^{14}C]DG (5 μCi) at t = 60 min, and blood samples (50 μL) were collected at t = −180, −5, 5, 10, 20, 30, 40, 50, 60, 65, 75, 85, 95, and 105 min. R_d is equal to R_a plus the glucose infusion rate (GIR) during the clamp period, whereas R_d is equal to R_a during the basal period. R_d and R_a were determined during the basal (t = −45 to 0 min) and clamp (t = 60 to 105 min) periods, as described previously (17). Immediately after collection of the final blood sample (t = 0 or 105 min), soleus muscle, red (Gastro Red) and white (Gastro White) portions of the gastrocnemius, heart, interscapular BAT, spleen, inguinal WAT (iWAT), epididymal WAT (eWAT), liver, and brain (cerebral cortex) were removed and frozen in liquid nitrogen. Gastro Red was dissected from the inner surface of the muscle attached to the soleus, whereas Gastro White was dissected from the outer surface of the muscle. The plasma concentration of insulin was measured at t = −5 and 105 min with the use of an ELISA kit (Shibayagi). Glycogen phosphorylase *a* activity in the liver was measured as described previously (17). We also determined GIR, R_a, and R_d in WT mice injected

intraperitoneally with saline as well as in CNO-injected SF1-Cre mice (without infection).

Food Intake

For measurement of food intake during refeeding after fasting, SF1-Cre:AAV-hM3Dq and SF1-Cre (without infection) mice were deprived of food overnight from 1700 to 0900 h, saline or CNO was injected intraperitoneally at 0830 h, and consumption of laboratory chow (CE-2) was determined during refeeding from 0900 to 1200 h. For measurement of food intake at the start of the dark period, saline or CNO was injected 30 min before the dark period (1730 h) into SF1-Cre:AAV-hM3Dq and SF1-Cre (without infection) mice fed ad libitum, and consumption of laboratory chow (CE-2) was measured over 3, 12, and 24 h after the start of the dark period.

Energy Expenditure, Locomotor Activity, and Respiratory Quotient

Energy expenditure and respiratory quotient (RQ) were measured by indirect calorimetry. Gas analysis was performed with a CO_2 and O_2 mass spectrometric analyzer (Arco-2000; Arco System, Chiba, Japan). Locomotor activity was measured with the use of a force plate system (Actracer-2000; Arco System) that was placed below the cage and which detects low-intensity activities (28). Mice were acclimatized to the analytic cage for 3 days before experiments. On the day of the experiment, SF1-Cre:AAV-hM3Dq mice were deprived of food at 0800 h ($t = -1$ h) and were injected with saline or CNO at 0900 h ($t = 0$). The VO_2 and VCO_2 as well as locomotor activity were measured every minute from 2100 h on the day before the experiment to 0900 h on the day after the start of the experiment (total of 36 h). The data were averaged for each consecutive 1-h period. Energy expenditure and the amount of carbohydrate or fat oxidized were calculated from VO_2 and VCO_2 as described previously (29) according to the following equations: energy expenditure ($cal \cdot min^{-1}$) = $(3.816 \times VO_2) + (1.231 \times VCO_2)$; carbohydrate oxidation ($cal \cdot min^{-1}$) = $([4.51 \times VCO_2] - [3.18 \times VO_2]) \times 4.1$; fat oxidation ($cal \cdot min^{-1}$) = $(1.67 \times [VO_2 - VCO_2]) \times 9.3$.

RNA Extraction and RT-PCR Analysis

Total RNA was isolated from tissue and subjected to reverse transcription as described previously (17). The resulting cDNA was analyzed by PCR or by quantitative PCR with SYBR Green PCR Mix (Takara Bio, Shiga, Japan) in an ABI 7500 real-time PCR system (Thermo Fisher Scientific, Yokohama, Japan). Data were normalized by the amount of 36B4 mRNA. The sequences of PCR primers are shown in the Supplementary Table 1.

Immunoblot Analysis

The extent of Akt phosphorylation was examined in soleus muscle and liver of SF1-Cre:AAV-hM3Dq mice injected with CNO or saline and subjected to a hyperinsulinemic-euglycemic clamp. It was also examined in soleus and liver of SF1-Cre:AAV-hM3Dq mice fed ad libitum and injected intraperitoneally first with saline or CNO at time $t = -180$ min and then with saline or insulin ($1 \text{ unit} \cdot kg^{-1}$) at $t = 0$, with the animals being sacrificed at $t = 10$ min by intraperitoneal injection of an overdose ($70 \text{ mg} \cdot kg^{-1}$) of pentobarbital sodium. Tissue samples were prepared as described previously (17) and were subjected to immunoblot analysis with antibodies specific for phosphorylated or total forms of Akt (Cell Signaling Technology Japan, Tokyo, Japan), horseradish peroxidase–conjugated secondary antibodies (Santa Cruz Biotechnology), and enhanced chemiluminescence reagents (GE Healthcare, Tokyo, Japan).

Electrophysiology

The brain was removed from 3- to 4-month-old SF1-Cre:AAV-hM3Dq or WT mice under deep anesthesia with isoflurane, and coronal slices of the hypothalamus (300 μm thick) were prepared and transferred to artificial cerebrospinal fluid (126 mmol/L NaCl, 3 mmol/L KCl, 1.3 mmol/L $MgSO_4$, 2.4 mmol/L $CaCl_2$, 1.2 mmol/L NaH_2PO_4, 26 mmol/L $NaHCO_3$, 10 mmol/L glucose) at 33°C, as described previously (30). To reduce spontaneous firing of hypothalamic neurons during recording, we lowered the glucose concentration in the artificial cerebrospinal fluid to 5 mmol/L. SF1 neurons in the VMH labeled with mCherry were targeted by patch pipettes with the use of a BX51 microscope (Olympus) under fluorescent and infrared differential interference contrast optics. The patch pipettes (4 to 6 MΩ) were filled with a solution containing 130 mmol/L potassium gluconate, 8 mmol/L KCl, 1 mmol/L $MgCl_2$, 0.6 mmol/L EGTA, 10 mmol/L HEPES, 3 mmol/L ATP (Mg^{2+} salt), 0.5 mmol/L guanosine-5'-triphosphate (disodium salt), and 10 mmol/L sodium phosphocreatine (adjusted to pH 7.3 with KOH). Membrane potentials were recorded in the current-clamp mode at a sampling rate of 10 kHz with the use of a Multiclamp 700B amplifier (Molecular Devices, Sunnyvale, CA). Tetrodotoxin (1 μmol/L) was added as indicated to block action potentials. We selected cells with a high seal resistance (>1 GΩ) and a low series resistance (<25 MΩ) for analysis. After at least 5 min of stable recording, the recording was continued after bath application of CNO (1 μmol/L). To explore the effect of CNO on the activity of VMH neurons without hM3Dq expression, we examined the membrane potential of VMH neurons of WT mice in the absence or presence of CNO. Data are expressed as the average firing rate or membrane potential during 3 to 1 min before and 5 to 7 min after CNO application. A neuron was considered to be activated or inhibited when the firing rate was increased or decreased by ≥20%, respectively, or when the mean potential after CNO application was 2 SDs above and below the potential before CNO application, respectively.

Statistical Analysis

Quantitative data are presented for individual mice as means ± SD. Comparisons among multiple groups were performed with ANOVA, followed by the Tukey-Kramer post hoc test, and those between two groups were performed

with the paired or unpaired Student *t* test. A *P* value of <0.05 was considered statistically significant.

RESULTS

Expression of hM3Dq-mCherry in SF1 Neurons of the VMH and hM3Dq Activation by CNO

Consistent with the specific expression of SF1 in the VMH of the adult mouse brain (5–7), expression of the hM3Dq-mCherry fusion protein in the medial hypothalamus was limited to the VMH—being especially pronounced in the dorsomedial region of the nucleus—in SF1-Cre:AAV-hM3Dq mice (Fig. 1*A* and *B*). In contrast, the fusion protein was not expressed in WT mice injected with the AAV-hM3Dq vector (Fig. 1*A*). CNO injection showed a larger number of cfos and hM3Dq-positive SF1 neurons in the unilateral side of the VMH expressing hM3Dq, being especially in the dorsomedial region of the VMH, compared with that in the contralateral (control) side of the VMH without hM3Dq expression (Fig. 1*C*). Saline injection did not show any cfos and hM3Dq-postive neurons in SF1-Cre:AAV-hM3Dq mice (data not shown). These results suggested that CNO activates SF1 neurons expressing hM3Dq.

Patch-clamp recordings from fresh VMH slices prepared from SF1-Cre:AAV-hM3Dq mice revealed that bath application of the hM3Dq ligand CNO induced depolarization and increased the firing rate in most hM3Dq-mCherry–expressing SF1 neurons (Fig. 1*D* and *E*). Among 20 hM3Dq-mCherry–positive SF1 neurons examined, CNO increased the firing rate in 14 neurons, reduced it in 4 neurons, and had no effect in 2 neurons (Fig. 1*E*). The firing rate (mean ± SD) for all 20 neurons was 0.94 ± 1.00 Hz before and 2.00 ± 2.63 Hz after CNO application ($P < 0.05$). In the presence of the Na^+-channel blocker tetrodotoxin, CNO increased the membrane potential of all five hM3Dq-mCherry–expressing SF1 neurons examined from −47.7 ± 6.8 to −42.4 ± 7.5 mV ($P < 0.05$) (Fig. 1*D* and *F*). All tested neurons were thus depolarized by the application of CNO. Among 13 VMH neurons in WT mice, CNO increased the membrane potential in 1 neuron, decreased in 1 neuron, and had no effect in 11 neurons (Fig. 1*G*).

Activation of SF1 Neurons Reduces Food Intake

Given that electrical stimulation of the VMH was previously found to reduce food intake in rats (31), we examined the effect of intraperitoneal injection of CNO on food intake in SF1-Cre:AAV-hM3Dq and SF1-Cre (without AAV-hM3Dq infection) mice. CNO injection in SF1-Cre:AAV-hM3Dq mice reduced food intake during refeeding for 3 h after an overnight fast compared with the corresponding value for the same mice injected with saline (Fig. 2*A*). It also reduced food intake during the first 3 h of the dark period but not that measured over 12 or 24 h (Fig. 2*B* and *C*). CNO did not affect food intake in SF1-Cre mice (Fig. 2*A* and *B*). These results thus suggested that a single intraperitoneal injection of CNO in SF1-Cre:AAV-hM3Dq mice reduced food intake during the subsequent 3 h by acting at the hM3Dq receptor expressed in SF1 neurons of the VMH.

Activation of SF1 Neurons Increases Energy Expenditure

We next examined the effects of activation of SF1 neurons on energy expenditure, RQ, and locomotor activity. Compared with saline, CNO significantly increased hourly energy expenditure for the first 3 h after injection in SF1-Cre:AAV-hM3Dq mice (Fig. 3*A* and Supplementary Fig. 1), with total energy expenditure over the first 5 h also being significantly increased (Fig. 3*B*). Injection of CNO did not affect locomotor activity (Fig. 3*C* and *D*, and Supplementary Fig. 1), however, suggesting that the increased energy expenditure was independent of such activity. CNO reduced RQ compared with that observed after saline injection (Fig. 3*E* and Supplementary Fig. 1). It also increased VO_2 without affecting VCO_2 (Fig. 3*F* and *G* and Supplementary Fig. 1), and it increased fat oxidation without affecting carbohydrate oxidation (Fig. 3*H* and *I* and Supplementary Fig. 1). Together, these results thus suggested that activation of SF1 neurons in the VMH by DREADD technology increased energy expenditure and fat oxidation.

Activation of SF1 Neurons Increases Insulin Sensitivity in Some Peripheral Tissues

Activation of SF1 neurons by optogenetic stimulation with ChR2 was previously shown to induce hyperglycemia (10). We therefore examined whether activation of SF1 neurons by DREADD technology might have a similar effect. We found that CNO induced only a small, nonsignificant increase in the basal blood glucose level in SF1-Cre:AAV-hM3Dq mice (Fig. 4*A*). Performance of a GTT and ITT at 30 min after the CNO injection revealed that the effects of CNO on blood glucose and plasma insulin levels varied among experiments (data not shown). We previously showed that injection of leptin or a melanocortin receptor agonist into the VMH of mice increased insulin sensitivity in red-type skeletal muscle and liver (15–17), with these effects being apparent 3 to 6 h after the injection. We therefore examined the effects of CNO injection on GTT and ITT parameters at 3 h after the injection. Blood glucose levels during the GTT were significantly lower in mice injected with CNO than in the same animals injected with saline, whereas the plasma insulin concentration did not differ between the two treatments (Fig. 4*B* and *C*). Blood glucose levels during the ITT were also significantly lower for mice injected with CNO than in the same animals injected with saline, with the blood glucose concentration declining to ≤50 mg/dL in CNO-injected mice (Fig. 4*D*). Activation of SF1 neurons by the hM3Dq receptor thus increased glucose tolerance and insulin sensitivity in mice 3 h after the CNO injection.

It was possible that the circulating levels of gluconeogenic hormones, such as glucagon and glucocorticoids, might have been affected by the pronounced hypoglycemia induced during the ITT in CNO-injected mice. To prevent such a hypoglycemic response after insulin administration, we examined the effects of CNO injection in SF1-Cre:AAV-hM3Dq mice subjected to a hyperinsulinemic-euglycemic clamp beginning 3 h after the injection (Fig. 5*A*). We thus

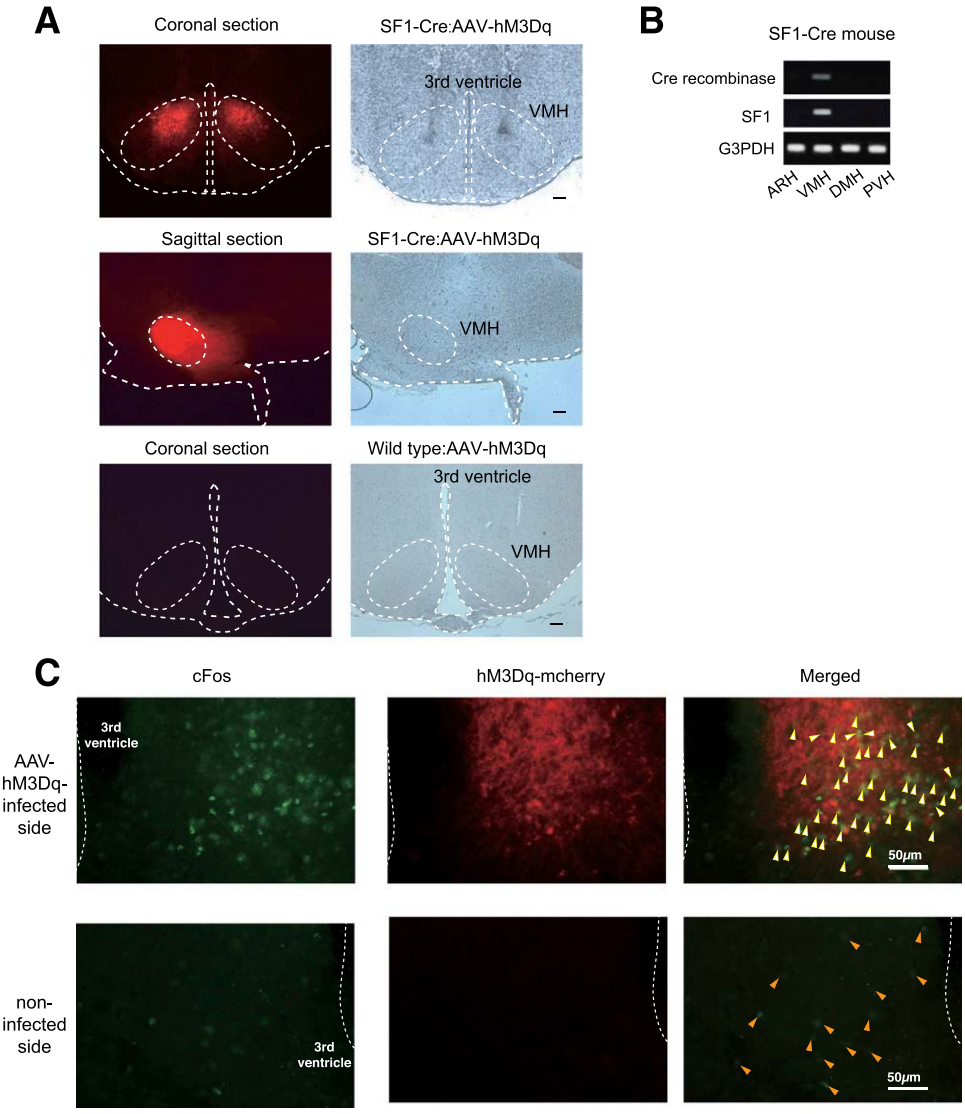

Figure 1—Expression of hM3Dq-mCherry in SF1 neurons of the VMH and electrophysiological validation of the DREADD system. *A*: Expression of hM3Dq-mCherry in SF1 neurons of the VMH of an SF1-Cre:AAV-hM3Dq mouse (coronal and sagittal sections) but not in those of a WT:AAV-hM3Dq mouse (coronal section) as revealed by the intrinsic fluorescence of mCherry (left images). Photomicrographs of the same hypothalamic sections are also shown (right images). Scale bars, 100 μm. *B*: RT-PCR analysis of Cre recombinase, SF1, and glyceraldehyde-3-phosphate dehydrogenase (G3PDH, internal control) mRNAs in the arcuate nucleus (ARH), VMH, and dorsomedial (DMH) and paraventricular (PVH) hypothalamus of SF1-Cre mice. *C*: cfos expression in the VMH of SF1-Cre mice. AAV-hM3Dq was infected into the unilateral side of the VMH. The yellow and orange arrowheads indicate a cfos-positive neuron with and without expression of hM3Dq, respectively. *D*: Representative recordings of action potentials (upper trace) and membrane potential (lower trace) from an hM3Dq-mCherry–expressing SF1 neuron in a freshly prepared tissue slice. The duration of bath application of CNO (1 μmol/L) is indicated by the bars. The membrane potential was recorded in the presence of tetrodotoxin (TTX). *E*: Firing rate (mean ± SD and individual neurons) of hM3Dq-mCherry–expressing SF1 neurons (n = 20) before and after application of CNO (left panel) as well as the relative change in the firing rate of individual neurons induced by CNO (right panel). Red, gray, and blue indicate neurons that show an increase (≥20%), no change (<20%), or decrease (≥20%) in the firing rate, respectively. *F*: Membrane potential of hM3Dq-mCherry–expressing SF1 neurons (n = 5) in the presence of TTX before and after application of CNO. Data are for individual neurons and mean ± SD (left) and Δ increase (right) of the membrane potential. *G*: Membrane potential of VMH neurons of WT mice before and after application of CNO (n = 13 neurons). Data are for individual neurons and mean ± SD (left) and Δ change (left) of the membrane potential. The black and white circles indicate neurons that show an increase or decrease (≥2 SDs) and no change (<2 SDs) in membrane potential, respectively. *P < 0.05 vs. before CNO application (paired Student t test).

initiated insulin and glucose infusion 3 h after CNO or saline injection in SF1-Cre:AAV-hM3Dq mice (Fig. 5*A*). The blood glucose concentration had not changed at 3 h after the CNO injection and was maintained during the hyperinsulinemic-euglycemic clamp at a level similar to that for the saline-injected control mice (Fig. 5*B*). However, the GIR was significantly higher after CNO injection than after saline injection (Fig. 5*C*), indicating that activation of SF1 neurons by the hM3Dq receptor increased whole-body insulin sensitivity during the clamp period.

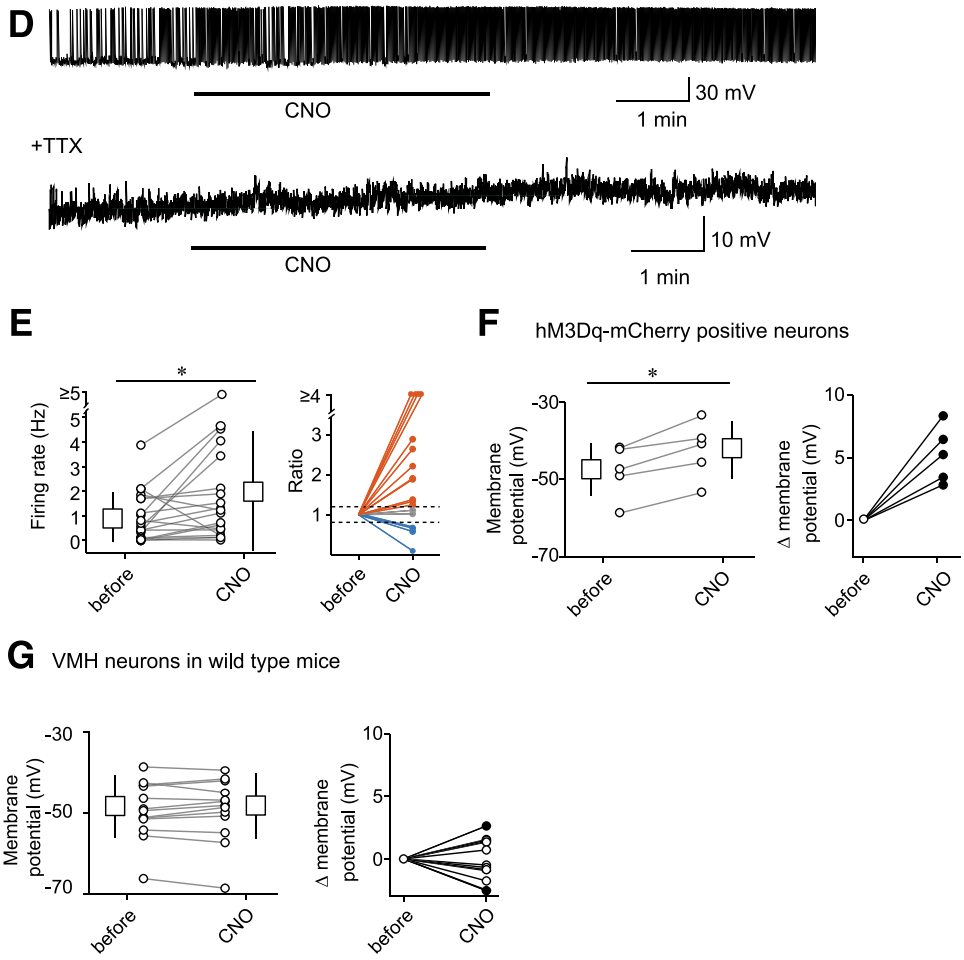

Figure 1—*Continued.*

The CNO-induced increase in GIR was associated with an increase in R_d during the clamp period (Fig. 5*D*). R_d was also increased during the basal period after CNO injection (Fig. 5*D*). Given that R_a is equal to R_d in the steady-state condition during the basal period, R_a was also increased during the basal period after CNO injection (Fig. 5*E*). CNO thus increased whole-body glucose turnover during the basal period. During the clamp period, R_a was significantly reduced in both saline- and CNO-injected mice but tended to be reduced to a greater extent after CNO injection (Fig. 5*E*). The plasma insulin concentration was increased approximately twofold during the clamp period compared with the basal period, with CNO injection tending to reduce the plasma insulin level during both basal and clamp periods compared with saline. These results suggested that activation of SF1 neurons in the VMH via the hM3Dq receptor enhanced whole-body insulin sensitivity under the hyperinsulinemic-euglycemic condition. There were no significant differences in blood glucose concentration, GIR, R_d, or R_a among saline-injected WT mice, CNO-injected SF1-Cre mice (without AAV-hM3Dq infection), and saline-injected SF1-Cre:AAV-hM3Dq mice (Supplementary Fig. 2), suggesting that the effects of CNO on glucose metabolism were mediated by hM3Dq expressed in SF1 neurons of the VMH.

We next examined 2DG uptake in the peripheral tissues of SF1-Cre:AAV-hM3Dq mice. CNO injection increased 2DG uptake during the basal period as well as enhanced insulin-induced glucose uptake during the clamp period in red-type skeletal muscle (soleus and Gastro Red), BAT, and heart, but not in Gastro White, spleen, eWAT, iWAT, or cerebral cortex (Fig. 6*A* and *B*).

Examination of the effect of CNO on insulin signaling in soleus muscle revealed that CNO increased the phosphorylation level of Akt, a key molecule of the insulin-signaling pathway, during the clamp period (Fig. 6*C*). Given that the insulin-induced increase in Akt phosphorylation is attenuated during insulin infusion, we examined the effect of acute insulin injection on Akt phosphorylation in soleus muscle of SF1-Cre:AAV-hM3Dq mice at 3 h after intraperitoneal injection of saline or CNO. CNO enhanced the insulin-induced phosphorylation of Akt in soleus muscle apparent 10 min after insulin injection without affecting the basal level of Akt phosphorylation (Fig. 6*D*).

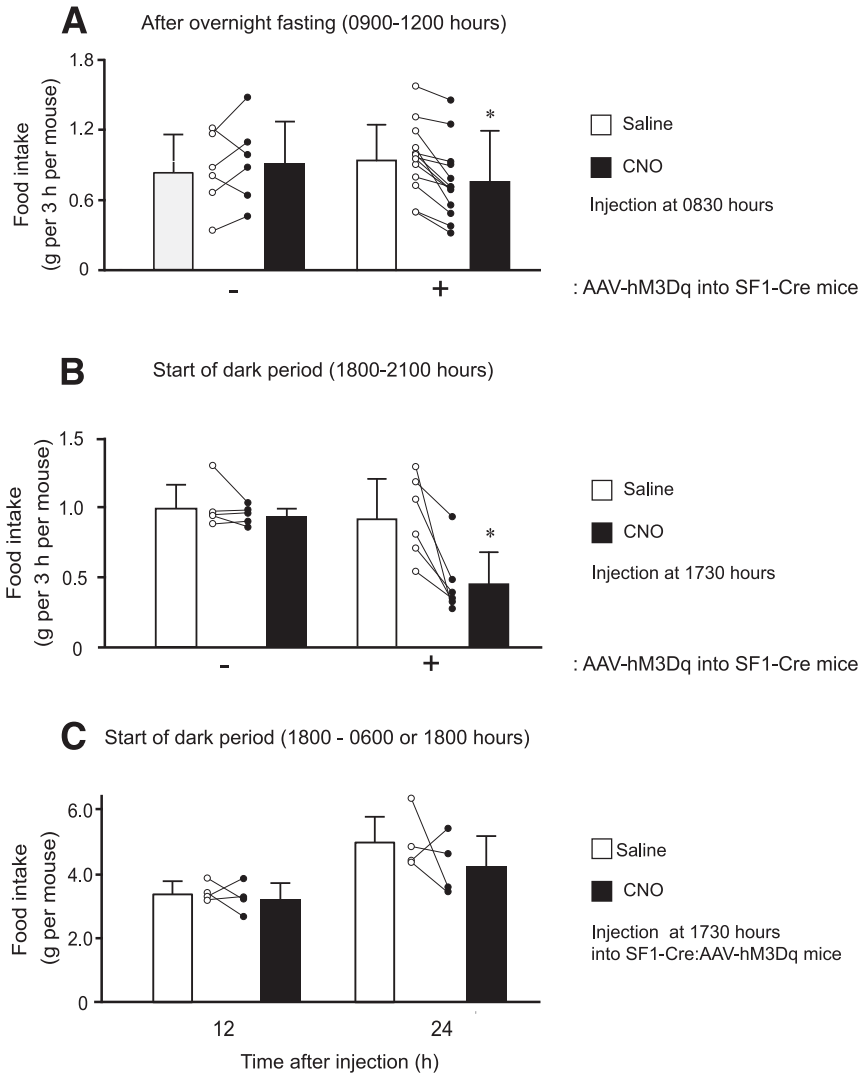

Figure 2—Activation of SF1 neurons reduces food intake. *A*: Food intake was measured over 3 h of refeeding with laboratory chow after an overnight fast for 16 h in SF1-Cre mice infected (n = 13) or not (n = 6) with AAV-hM3Dq. *B*: Food intake was measured during the first 3 h of the dark period with laboratory chow freely available in SF1-Cre mice infected (n = 6) or not (n = 5) with AAV-hM3Dq. *C*: Food intake was measured over 12 or 24 h after the start of the dark period with laboratory chow freely available in SF1-Cre:AAV-hM3Dq mice (n = 4). For all experiments, CNO or saline was injected intraperitoneally 30 min before measurement of food intake in the same mice on different days. Data are for individual mice and means ± SD. *P < 0.05 vs. corresponding value for saline injection.

To explore the mechanism by which activation of SF1 neurons by hM3Dq increases R_a during the basal period and why the effect of CNO is suppressed during the clamp period, we examined the effect of CNO injection on glycogen phosphorylase *a* activity in the liver of SF1-Cre:AAV-hM3Dq mice. CNO increased glycogen phosphorylase *a* activity in the liver during the basal period, and this effect of CNO was suppressed during the clamp period (Fig. 6*E*). These results suggested that activation of SF1 neurons in the VMH stimulates hepatic glucose production via activation of glycogen phosphorylase in the liver and thereby maintains blood glucose levels.

We also determined the effects of CNO on gluconeogenic gene expression in the liver of SF1-Cre:AAV-hM3Dq mice during the basal and clamp periods. In contrast to its effect on glycogen phosphorylase *a* activity, CNO injection reduced the amounts of glucose-6-phosphatase (G6Pase) and PEPCK mRNAs in the liver during the basal period and enhanced the insulin-induced downregulation of these mRNAs (Fig. 6*F* and *G*). Activation of SF1 neurons did not affect Akt phosphorylation during the clamp period or acute insulin-induced Akt phosphorylation in the liver (Fig. 6*H* and *I*). These results suggested that activation of SF1 neurons by DREADD technology suppressed gluconeogenic gene expression in the liver in an Akt-independent manner.

DISCUSSION

We have shown here that activation of SF1 neurons by DREADD technology with the designer receptor hM3Dq increased glucose uptake and insulin sensitivity in red-type

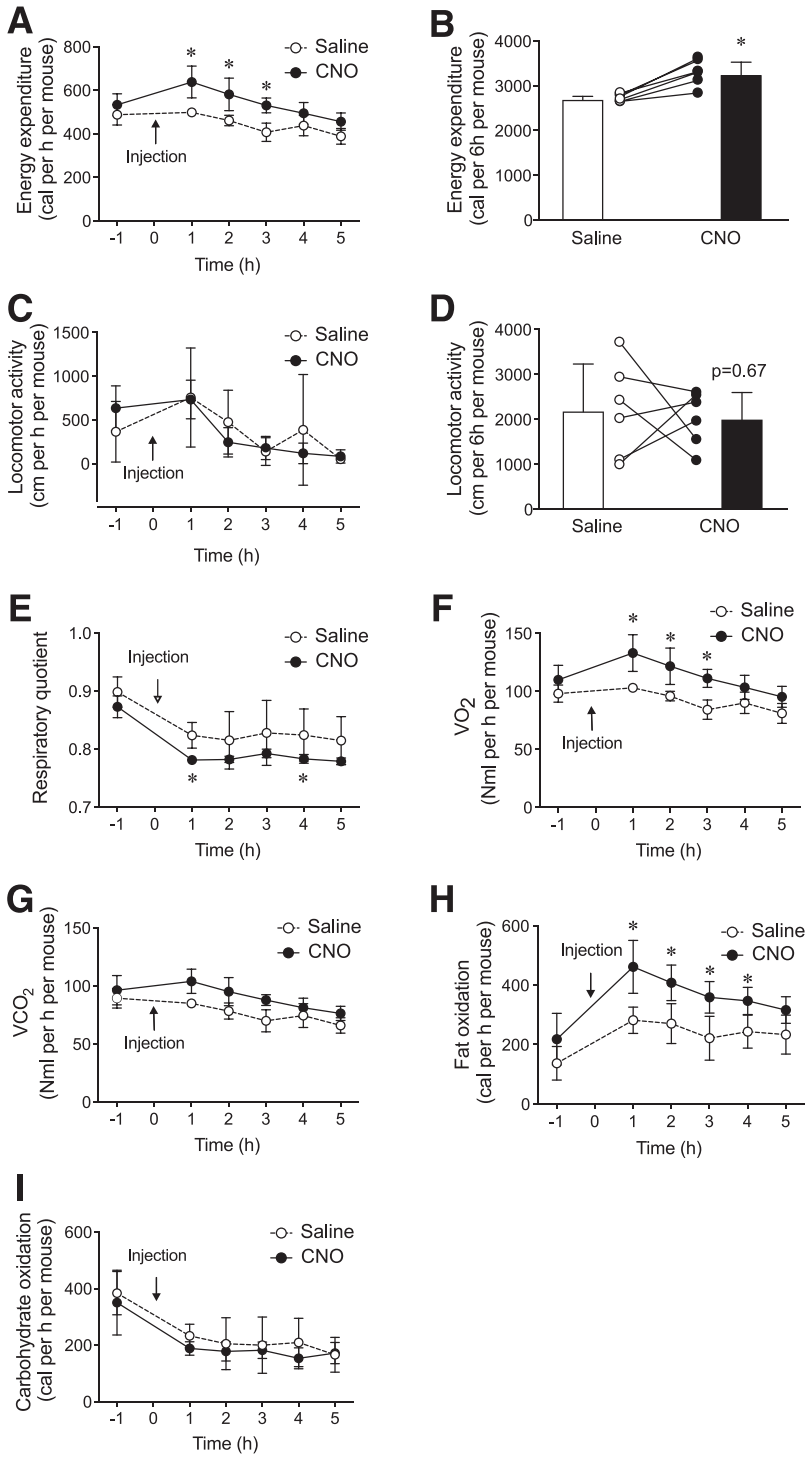

Figure 3—Activation of SF1 neurons increases energy expenditure and fat oxidation. SF1-Cre:AAV-hM3Dq mice were deprived of food for 1 h and then injected intraperitoneally with CNO or saline (same animals, different days) at $t = 0$ for measurement of energy expenditure (*A*), locomotor activity (*C*), RQ (*E*), VO_2 (*F*), VCO_2 (*G*), fat oxidation (*H*), and carbohydrate oxidation (*I*). Total energy expenditure (*B*) and locomotor activity (*D*) over 6 h were also calculated. Data are means ± SD ($n = 6$). Bar graphs also show the data for individual mice. *$P < 0.05$ vs. corresponding saline value. See Supplementary Fig. 1 for measurements over 36 h.

skeletal muscle, BAT, and heart. We also found that activation of SF1 neurons by hM3Dq maintained euglycemia under basal conditions, in contrast to the hyperglycemic effect of activation either of SF1 neurons by ChR2 (10) or of GK-expressing neurons in the VMH by TRPV1 (9). Activation of SF1 neurons by hM3Dq increased glycogen phosphorylase *a* activity in the liver, whereas this effect was suppressed during a hyperinsulinemic-euglycemic clamp.

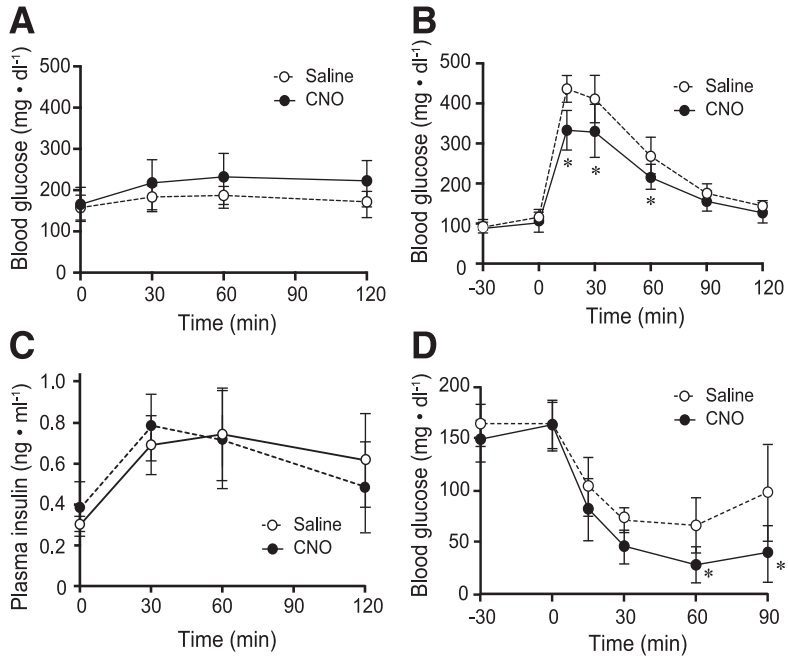

Figure 4—Effects of activation of SF1 neurons on blood glucose level, GTT, and ITT. *A*: Basal blood glucose level after intraperitoneal injection of saline or CNO at $t = 0$ min in the same SF1-Cre:AAV-hM3Dq mice ($n = 9$) on different days. The mice were deprived of food for 3 h before measurements. Blood glucose (*B*) and plasma insulin (*C*) levels during a GTT performed 3 h after intraperitoneal injection of saline or CNO in the same SF1-Cre:AAV-hM3Dq mice ($n = 5$) on different days. Mice were deprived of food overnight before the test, and glucose (2 g · kg^{-1}) was injected intraperitoneally at $t = 0$. *D*: Blood glucose level during an ITT performed 3 h after intraperitoneal injection of saline or CNO in the same SF1-Cre:AAV-hM3Dq mice ($n = 7$) on different days. Mice were fed ad libitum until the injection of saline or CNO, and insulin (1 unit · kg^{-1}) was injected intraperitoneally at $t = 0$. All data are means ± SD. *$P < 0.05$ vs. corresponding value for saline injection.

These results suggest that activation of SF1 neurons by hM3Dq increases hepatic glucose production by activation of glycogen phosphorylase *a* in this tissue and thereby maintains blood glucose levels. We also found that activation of SF1 neurons by DREADD technology downregulated the hepatic abundance of mRNAs for gluconeogenic genes and that this effect was enhanced under the hyperinsulinemic-euglycemic condition. The activation of SF1 neurons by hM3Dq thus has two distinct effects on glucose metabolism in the liver: it increases glycogen phosphorylase *a* activity, and it inhibits gluconeogenic gene expression. Together, our observations suggest that activation of SF1 neurons by hM3Dq increases glucose uptake in peripheral tissues, including red-type skeletal muscle, BAT, and heart, as well as glucose production in the liver. It also promotes insulin-induced glucose uptake in these peripheral tissues and insulin-induced suppression of gluconeogenic gene expression in the liver. We also found that activation of SF1 neurons via DREADD technology reduced food intake and increased energy expenditure.

SF1 neurons are regulated by humoral factors such as nutrients (e.g., glucose) and hormones (e.g., leptin and insulin) (8,12–14,19,22–24). The long form of the leptin receptor is expressed in some VMH neurons (18), and leptin increases the activity of a subset of SF1 neurons in the VMH (12–14). Leptin promotes glucose uptake and insulin sensitivity in peripheral tissues, including red-type skeletal muscle, BAT, and heart via VMH neurons, maintaining blood glucose levels through increased hepatic glucose production (15–17), and it promotes insulin-induced suppression of hepatic glucose production through a distinct mechanism in the VMH (17). Our present data now suggest that activation of Gq signaling in SF1 neurons by hM3Dq mimics the effects of leptin on glucose and energy metabolism but does not trigger a hyperglycemic response. These observations suggest that a subset of SF1 neurons increases insulin sensitivity in peripheral tissues, whereas another subset of SF1 neurons induces hyperglycemia and enhances the counterregulatory response to glucopenia. A previous study also suggested that hM3Dq may regulate distinct types of neurons compared with those regulated by an optogenetic approach (25). Ligation of hM3Dq may therefore activate a subset of SF1 neurons in the VMH that includes leptin receptor–expressing neurons. We have shown that injection of glutamate into the VMH induced hyperglycemia as well as glucose uptake in some peripheral tissues, including red-type skeletal muscle, heart, and BAT (11). Activation of ionotropic glutamate receptors in SF1 neurons may thus induce both a hyperglycemic response and glucose uptake in these peripheral tissues. Similarly, activation of SF1 neurons by ChR2 may induce glucose uptake preferentially in some peripheral tissues as well as hyperglycemia. However, it is also possible that the distinct effects of optogenetic and DREADD stimulation on glucose metabolism

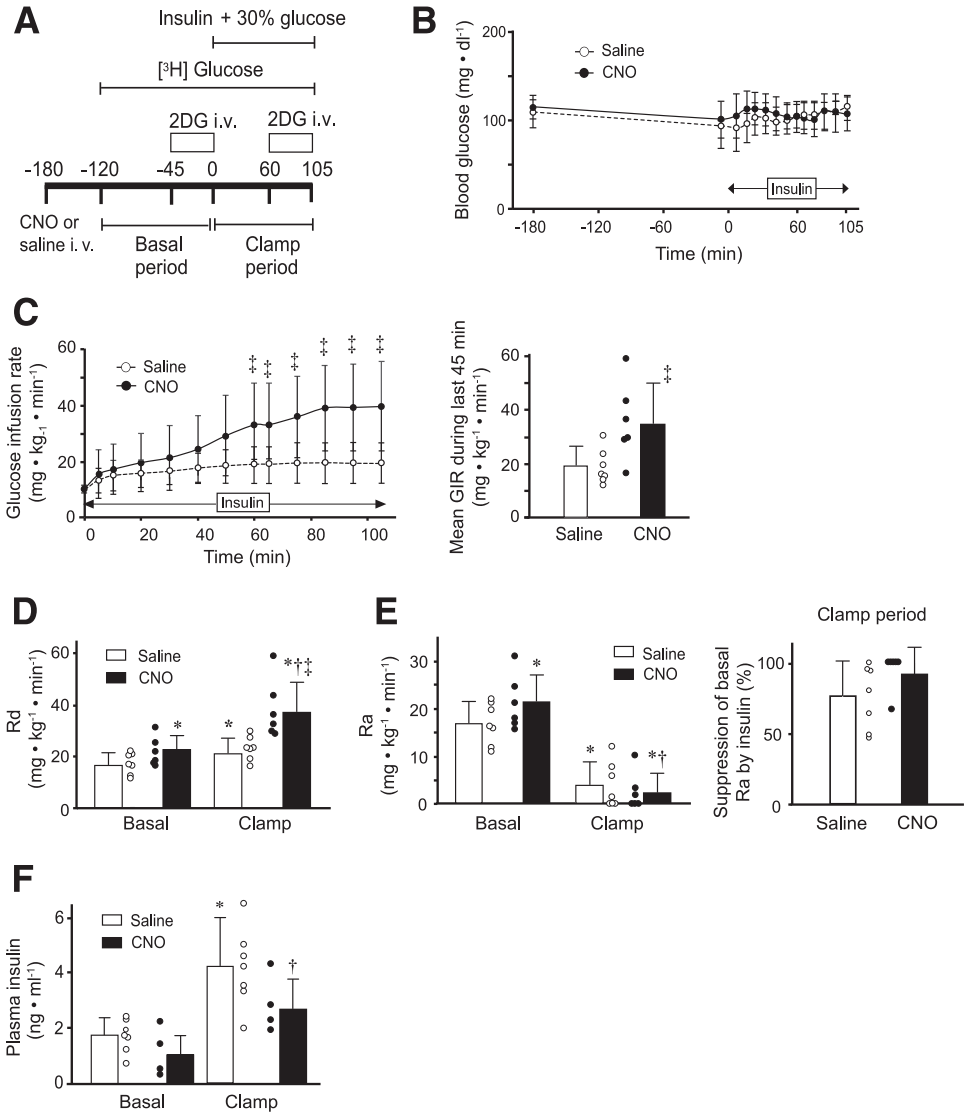

Figure 5—Activation of SF1 neurons increases whole-body insulin sensitivity. *A*: Experimental protocol for the hyperinsulinemic-euglycemic clamp and measurement of 2DG uptake. SF1-Cre:AAV-hM3Dq mice were injected intravenously (i.v.) with saline or CNO at $t = -180$ min. *B*: Blood glucose concentration before and after insulin infusion for the hyperinsulinemic-euglycemic clamp. *C*: GIR during the hyperinsulinemic-euglycemic clamp (left panel) and mean GIR during the final 45 min of the clamp period (right panel). *D*: Glucose R_d during the basal and clamp periods. *E*: Glucose R_a during the basal and clamp periods (left panel) as well as the percentage suppression of R_a induced by the insulin infusion (right panel). *F*: Plasma insulin level during the basal and clamp periods. All data are means ± SD for mice injected with saline ($n = 7$) and CNO ($n = 6$), with the exception of mice injected with CNO in panel *F* ($n = 4$). Bar graphs also show the data for individual mice. *$P < 0.05$ vs. saline injection and basal period; †$P < 0.05$ vs. CNO injection and basal period; ‡$P < 0.05$ vs. saline injection and clamp period.

result from the different expression of hM3Dq and ChR2 in a specific region of the VMH. In the current study, hM3Dq was expressed at a high level in the dorsomedial region of the VMH. Most leptin-activated SF1 neurons are located within the dorsomedial subdivision of the VMH (14).

Activation of SF1 neurons in the VMH increased phosphorylation of Akt in soleus muscle during the hyperinsulinemic-euglycemic clamp as well as enhanced that induced by acute injection of insulin. We previously showed that activation of VMH neurons by orexin, acting via muscle sympathetic nerves and β_2-adrenergic receptors, stimulates glucose uptake and insulin sensitivity in red-type skeletal muscle by increasing insulin delivery from blood vessels (32). Activation of SF1 neurons by DREADD technology may thus increase insulin sensitivity in red-type skeletal muscle also by enhancing insulin delivery to muscle cells. In contrast, we have shown that electrical stimulation of the VMH promotes glucose transport in heart muscle and BAT by influencing different aspects of insulin action (33). Similarly, CNO did not affect Akt phosphorylation in soleus muscle of mice without insulin infusion. Activation of SF1 neurons in the VMH may therefore increase glucose uptake in red-type skeletal muscle, heart, and BAT in both insulin-independent and -dependent manners.

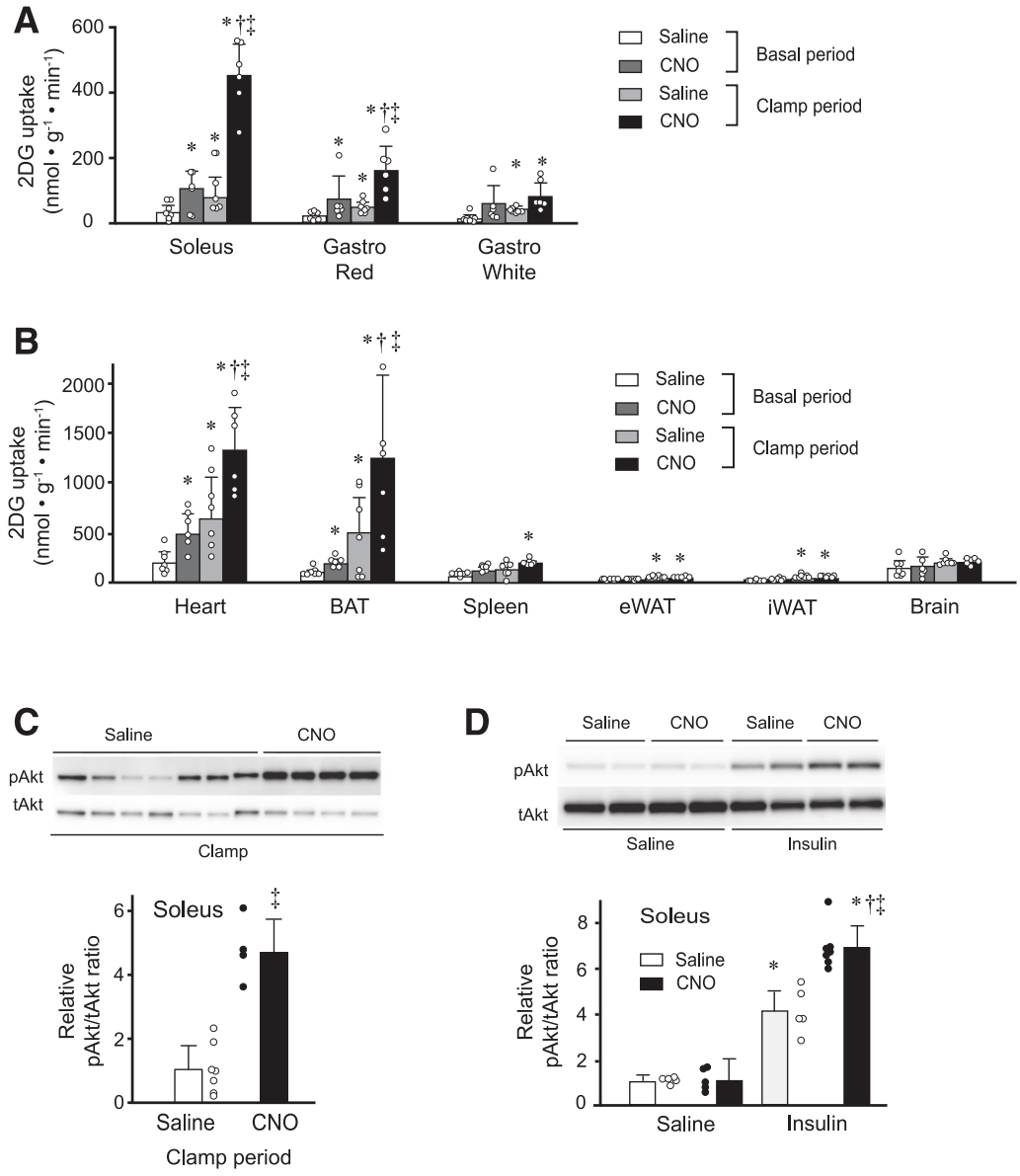

Figure 6—Activation of SF1 neurons increases insulin sensitivity in peripheral tissues. Rates of 2DG uptake in skeletal muscle (soleus, Gastro Red, Gastro White) (*A*) and heart, interscapular BAT, spleen, eWAT, iWAT, and brain (cerebral cortex) (*B*) of SF1-Cre:AAV-hM3Dq mice injected with saline ($n = 7$) or CNO ($n = 6$). Data are shown for basal and clamp periods. *C*: Immunoblot analysis of the relative ratio of phosphorylated (p) to total (t) forms of Akt in soleus muscle during the clamp period for SF1-Cre:AAV-hM3Dq mice injected with saline ($n = 7$) or CNO ($n = 4$). *D*: Representative immunoblot analysis and quantitation of the relative pAkt-to-tAkt ratio in soleus of SF1-Cre:AAV-hM3Dq mice at 30 min after intraperitoneal injection of insulin (1 unit · kg^{-1}) or saline. CNO (or saline) was injected intraperitoneally 180 min before the insulin (or saline) injection. With the exception of CNO + insulin ($n = 7$), $n = 5$ mice for each group. *E*: Glycogen phosphorylase *a* activity in the liver during basal and clamp periods for SF1-Cre:AAV-hM3Dq mice injected with saline ($n = 7$) or CNO ($n = 5$). RT-quantitative PCR analysis of the relative amounts of G6Pase (*F*) and PEPCK (*G*) mRNAs during the basal and clamp periods for SF1-Cre:AAV-hM3Dq mice injected with saline ($n = 7$) or CNO ($n = 4$). *H*: Immunoblot analysis of the relative pAkt-to-tAkt ratio in the liver during the clamp period for SF1-Cre:AAV-hM3Dq mice injected with saline ($n = 5$) or CNO ($n = 4$). *I*: Representative immunoblot analysis and quantitation of the relative pAkt-to-tAkt ratio in the liver of SF1-Cre:AAV-hM3Dq mice at 30 min after an intraperitoneal injection of insulin (1 unit · kg^{-1}) or saline. CNO (or saline) was injected intraperitoneally 180 min before the insulin (or saline) injection. With the exception of CNO + insulin ($n = 7$), $n = 5$ mice for each group. All quantitative data are for individual mice and means ± SD. *$P < 0.05$ vs. saline injection and basal period or saline + saline; †$P < 0.05$ vs. CNO injection and basal period or CNO + saline; ‡$P < 0.05$ vs. saline injection and clamp period or saline + insulin.

Activation of SF1 neurons by DREADD technology increased glycogen phosphorylase *a* activity in the liver under basal conditions but suppressed hepatic expression of the gluconeogenic genes for G6Pase and PEPCK. The extent of Akt phosphorylation in the liver was not affected by injection of CNO with or without insulin infusion. These results suggest that activation of SF1 neurons by hM3Dq regulates hepatic glycogenolysis and gluconeogenesis in an Akt-independent manner. Intracerebroventricular injection of leptin was also previously shown to regulate hepatic

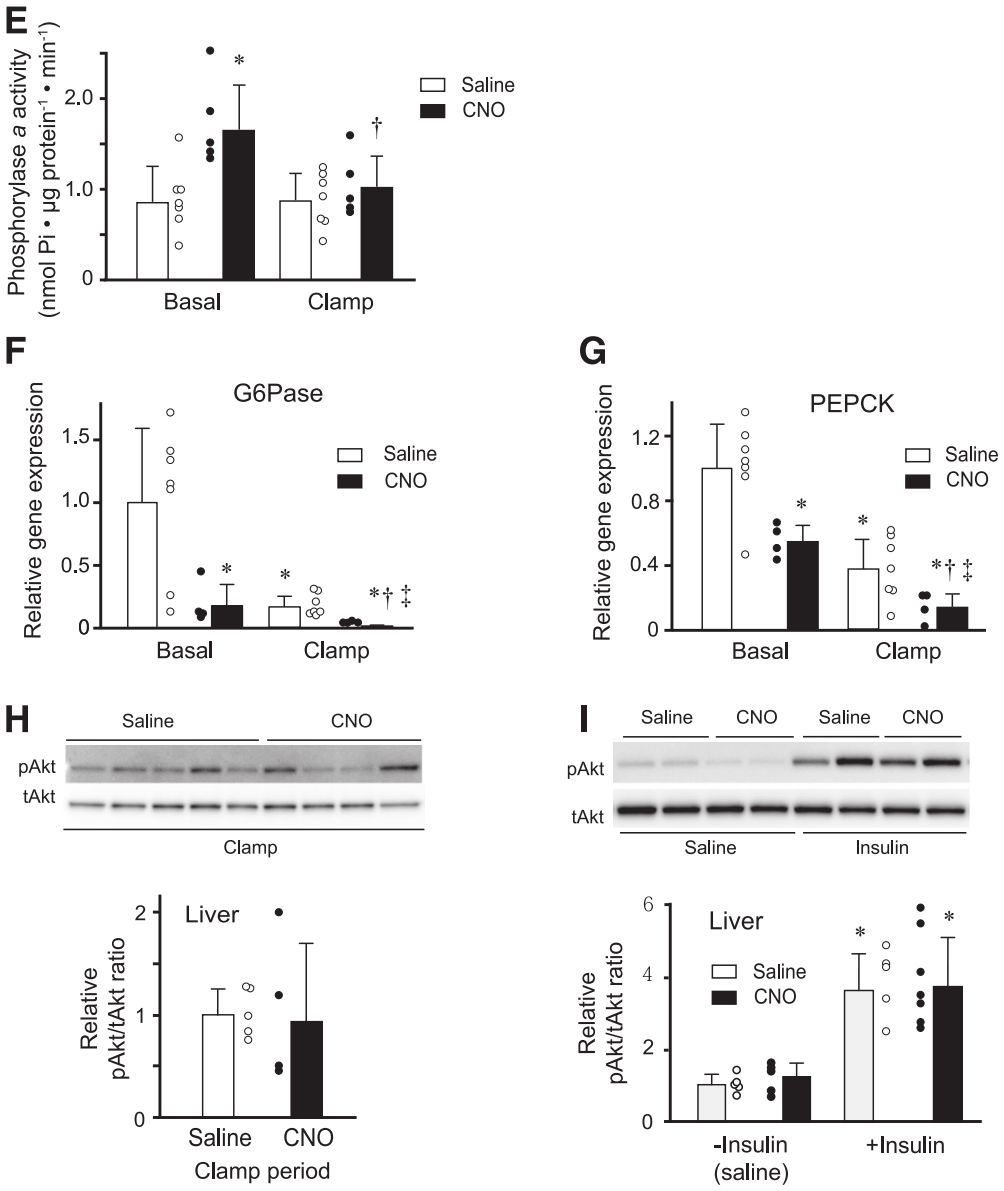

Figure 6—*Continued.*

glycogenolysis and gluconeogenesis in a reciprocal manner (34). Further study is warranted to explore the mechanisms by which activation of SF1 neurons by hM3Dq regulates glucose metabolism in the liver.

Activation of SF1 neurons by hM3Dq suppressed food intake not only at the start of the dark period but also after an overnight fast, suggesting that activation of these neurons in the VMH via this receptor promotes satiety. A locus in the VMH—especially in the ventrolateral region of the nucleus—has been shown to promote aggressive behavior (35), and the VMH neurons responsible for this effect are marked by expression of estrogen receptor 1 (Esr1) (36). However, we did not detect any aggression-like behavior after injection of CNO in SF1-Cre:AAV-hM3Dq mice (data not shown). In the current study, hM3Dq was expressed at a high level in the dorsomedial region of the VMH, while Esr1 is expressed in the ventrolateral region of the VMH (36). Thus, CNO did possibly not activate Esr1 expressing neurons in the ventrolateral region of the VMH. We also found that activation of SF1 neurons by hM3Dq increased energy expenditure without altering locomotor activity, with this effect being the result of increased fat oxidation. These results are consistent with our previous data showing that leptin stimulates fatty acid oxidation in red-type skeletal muscle via activation of muscle AMPK (37).

The VMH contains glucose-excitatory and glucose-inhibitory neurons (13,14,38). Activation of glucose-excitatory neurons among SF1 neurons in the VMH was recently shown to regulate insulin sensitivity in skeletal muscle and the liver via uncoupling protein 2 (UCP2) and mitochondrial fission

(39). Among glucose-excitatory neurons in the VMH, the number of cells excited by leptin is almost twice that of those inhibited by leptin (13). Further studies are necessary to explore the effects of hM3Dq activation on glucose-excitatory, glucose-inhibitory, and leptin receptor–expressing neurons in the VMH. Collectively, our results show that DREADD technology provides an important tool for investigations of the role of the central nervous system in the control of insulin sensitivity and glucose metabolism in peripheral tissues.

Acknowledgments. The authors thank Pavel Osten (Cold Spring Harbor Laboratory, Cold Spring Harbor, NY) and Bryan L. Roth (Department of Pharmacology and National Institute of Mental Health Psychoactive Drug Screening Program, University of North Carolina School of Medicine, Chapel Hill, NC) for viral vectors, Megumi Hayashi (Division of Endocrinology and Metabolism, National Institute for Physiological Sciences) for help with manuscript preparation, Rie Kageyama (Section of Viral Vector Development, Center for Genetic Analysis of Behavior, National Institute for Physiological Sciences) for virus preparation, the Functional Genomics Facility at the National Institute for Basic Biology for DNA sequencing, and the Center for Radioisotope Facilities at the National Institute for Basic Biology for assistance with radioisotope experiments.

Funding. This study was supported by the following grants from the Japan Society for the Promotion of Science: Grant-in-Aid for Scientific Research (C) (15K09405) to S.O., Grant-in-Aid for Scientific Research (B) (24390058) to Y.M., and Grant-in-Aid for Exploratory Research (15K15352) to Y.M. The study was supported by the Ministry of Education, Culture, Sports, Science, and Technology of Japan through a Grant-in-Aid for Scientific Research on Innovative Areas (22126005) to Y.M. and by the Core Research for Evolutional Science and Technology Program AMED-CREST of the Japan Science and Technology Agency and the Japan Agency for Medical Research and Development to Y.M.

Duality of Interest. No potential conflicts of interest relevant to this article were reported.

Author Contributions. E.A.C. performed GTT and hyperinsulinemic-euglycemic clamp analyses. E.A.C. and S.O. performed the ITT and histological experiments. E.A.C., S.O., T.S., and K.K. prepared and evaluated viral vectors. E.A.C., S.Y., K.S., and C.-C.W. performed biochemical experiments. E.A.C. and K.T. performed energy expenditure experiments. E.A.C. and Y.M. designed the experiments, analyzed the data, and wrote the manuscript. A.W.I. and Y.Y. performed electrophysiological experiments. N.W., T.H., and S.S. supervised the histological experiments. Y.O. supervised the project. Y.M. is the guarantor of this work and, as such, had full access to all the data in the study and takes responsibility for the integrity of the data and the accuracy of the data analysis.

References

1. Swanson LW. The hypothalamus. In *Integrated Systems of the CNS, Part I: Hypothalamus, Hippocampus, Amygdala, Retina (Handbook of Chemical Neuroanatomy), Handbook of Chemical Neuroanatomy*. Vol 5. Björklund A, Hökfelt T, Swanson LW, Eds. Amsterdam, Elsevier Science, 1987, p. 1-124

2. Grayson BE, Seeley RJ, Sandoval DA. Wired on sugar: the role of the CNS in the regulation of glucose homeostasis. Nat Rev Neurosci 2013;14:24–37

3. Morton GJ, Schwartz MW. Leptin and the central nervous system control of glucose metabolism. Physiol Rev 2011;91:389–411

4. Shimazu T, Fukuda A, Ban T. Reciprocal influences of the ventromedial and lateral hypothalamic nuclei on blood glucose level and liver glycogen content. Nature 1966;210:1178–1179

5. Majdic G, Young M, Gomez-Sanchez E, et al. Knockout mice lacking steroidogenic factor 1 are a novel genetic model of hypothalamic obesity. Endocrinology 2002;143:607–614

6. Zhao L, Bakke M, Hanley NA, et al. Tissue-specific knockouts of steroidogenic factor 1. Mol Cell Endocrinol 2004;215:89–94

7. Shima Y, Zubair M, Ishihara S, et al. Ventromedial hypothalamic nucleus-specific enhancer of Ad4BP/SF-1 gene. Mol Endocrinol 2005;19:2812–2823

8. Tong Q, Ye C, McCrimmon RJ, et al. Synaptic glutamate release by ventromedial hypothalamic neurons is part of the neurocircuitry that prevents hypoglycemia. Cell Metab 2007;5:383–393

9. Stanley SA, Kelly L, Latcha KN, et al. Bidirectional electromagnetic control of the hypothalamus regulates feeding and metabolism. Nature 2016;531:647–650

10. Meek TH, Nelson JT, Matsen ME, et al. Functional identification of a neurocircuit regulating blood glucose. Proc Natl Acad Sci U S A 2016;113:E2073–E2082

11. Sudo M, Minokoshi Y, Shimazu T. Ventromedial hypothalamic stimulation enhances peripheral glucose uptake in anesthetized rats. Am J Physiol 1991;261:E298–E303

12. Dhillon H, Zigman JM, Ye C, et al. Leptin directly activates SF1 neurons in the VMH, and this action by leptin is required for normal body-weight homeostasis. Neuron 2006;49:191–203

13. Irani BG, Le Foll C, Dunn-Meynell A, Levin BE. Effects of leptin on rat ventromedial hypothalamic neurons. Endocrinology 2008;149:5146–5154

14. Sohn JW, Oh Y, Kim KW, Lee S, Williams KW, Elmquist JK. Leptin and insulin engage specific PI3K subunits in hypothalamic SF1 neurons. Mol Metab 2016;5:669–679

15. Minokoshi Y, Haque MS, Shimazu T. Microinjection of leptin into the ventromedial hypothalamus increases glucose uptake in peripheral tissues in rats. Diabetes 1999;48:287–291

16. Toda C, Shiuchi T, Lee S, et al. Distinct effects of leptin and a melanocortin receptor agonist injected into medial hypothalamic nuclei on glucose uptake in peripheral tissues. Diabetes 2009;58:2757–2765

17. Toda C, Shiuchi T, Kageyama H, et al. Extracellular signal-regulated kinase in the ventromedial hypothalamus mediates leptin-induced glucose uptake in red-type skeletal muscle. Diabetes 2013;62:2295–2307

18. Elmquist JK, Bjørbaek C, Ahima RS, Flier JS, Saper CB. Distributions of leptin receptor mRNA isoforms in the rat brain. J Comp Neurol 1998;395:535–547

19. Bingham NC, Anderson KK, Reuter AL, Stallings NR, Parker KL. Selective loss of leptin receptors in the ventromedial hypothalamic nucleus results in increased adiposity and a metabolic syndrome. Endocrinology 2008;149:2138–2148

20. Zhang R, Dhillon H, Yin H, et al. Selective inactivation of Socs3 in SF1 neurons improves glucose homeostasis without affecting body weight. Endocrinology 2008;149:5654–5661

21. Xu Y, Hill JW, Fukuda M, et al. PI3K signaling in the ventromedial hypothalamic nucleus is required for normal energy homeostasis. Cell Metab 2010;12:88–95

22. Klöckener T, Hess S, Belgardt BF, et al. High-fat feeding promotes obesity via insulin receptor/PI3K-dependent inhibition of SF-1 VMH neurons. Nat Neurosci 2011;14:911–918

23. Kim KW, Zhao L, Donato J Jr, et al. Steroidogenic factor 1 directs programs regulating diet-induced thermogenesis and leptin action in the ventral medial hypothalamic nucleus. Proc Natl Acad Sci U S A 2011;108:10673–10678

24. Meek TH, Matsen ME, Dorfman MD, et al. Leptin action in the ventromedial hypothalamic nucleus is sufficient, but not necessary, to normalize diabetic hyperglycemia. Endocrinology 2013;154:3067–3076

25. Alexander GM, Rogan SC, Abbas AI, et al. Remote control of neuronal activity in transgenic mice expressing evolved G protein-coupled receptors. Neuron 2009;63:27–39

26. Paxinos G, Franklin K. *The Mouse Brain in Stereotaxic Coordinates*. 3rd ed. San Diego, CA, Academic Press, 2007

27. Krashes MJ, Koda S, Ye C, et al. Rapid, reversible activation of AgRP neurons drives feeding behavior in mice. J Clin Invest 2011;121:1424–1428

28. Virtue S, Even P, Vidal-Puig A. Below thermoneutrality, changes in activity do not drive changes in total daily energy expenditure between groups of mice. Cell Metab 2012;16:665–671

29. Ishihara K, Oyaizu S, Onuki K, Lim K, Fushiki T. Chronic (-)-hydroxycitrate administration spares carbohydrate utilization and promotes lipid oxidation during exercise in mice. J Nutr 2000;130:2990–2995
30. Ishikawa AW, Komatsu Y, Yoshimura Y. Experience-dependent emergence of fine-scale networks in visual cortex. J Neurosci 2014;34:12576–12586
31. Beltt BM, Keesey RE. Hypothalamic map of stimulation current thresholds for inhibition of feeding in rats. Am J Physiol 1975;229:1124–1133
32. Shiuchi T, Haque MS, Okamoto S, et al. Hypothalamic orexin stimulates feeding-associated glucose utilization in skeletal muscle via sympathetic nervous system. Cell Metab 2009;10:466–480
33. Takahashi A, Sudo M, Minokoshi Y, Shimazu T. Effects of ventromedial hypothalamic stimulation on glucose transport system in rat tissues. Am J Physiol 1992;263:R1228–R1234
34. Liu L, Karkanias GB, Morales JC, et al. Intracerebroventricular leptin regulates hepatic but not peripheral glucose fluxes. J Biol Chem 1998;273:31160–31167
35. Lin D, Boyle MP, Dollar P, et al. Functional identification of an aggression locus in the mouse hypothalamus. Nature 2011;470:221–226
36. Lee H, Kim DW, Remedios R, et al. Scalable control of mounting and attack by $Esr1^{+}$ neurons in the ventromedial hypothalamus. Nature 2014;509:627–632
37. Minokoshi Y, Kim YB, Peroni OD, et al. Leptin stimulates fatty-acid oxidation by activating AMP-activated protein kinase. Nature 2002;415:339–343
38. Kang L, Dunn-Meynell AA, Routh VH, et al. Glucokinase is a critical regulator of ventromedial hypothalamic neuronal glucosensing. Diabetes 2006;55:412–420
39. Toda C, Kim JD, Impellizzeri D, Cuzzocrea S, Liu ZW, Diano S. UCP2 regulates mitochondrial fission and ventromedial nucleus control of glucose responsiveness. Cell 2016;164:872–883